



# OPEN The MiR-139-5p and CXCR4 axis may play a role in high glucose-induced inflammation by regulating monocyte migration

Weifang Li<sup>1,2</sup>, Gengchen Xu<sup>2</sup>, Gregory W. Chai<sup>2</sup>, Alexander Ball<sup>2</sup>, Qiuwang Zhang<sup>2</sup>✉ & Michael J. B. Kutryk<sup>2</sup>✉

MicroRNAs, a class of small non-coding RNA molecules that regulate gene expression post-transcriptionally, are implicated in various pathological conditions including diabetes mellitus (DM). DM has been increasingly recognized as an inflammatory disease and monocytes play a key role in propagating inflammation under hyperglycemic conditions. We hypothesize that high glucose dysregulates microRNAs to promote monocyte inflammatory activity, which may contribute to the pathogenesis of DM. THP-1 monocytes were cultured in normal (5 mM) and high (25 mM) glucose conditions. RT-qPCR and Western blotting were performed to assay microRNAs and proteins, respectively. Monocytes were transfected with microRNA mimics using Lipofectamine RNAiMAX reagent. THP-1 monocyte growth was assessed using Calcein-AM dye and a Boyden chamber assay was applied to measure monocyte migration. The results showed that high glucose downregulated miR-139-5p associated with increased protein expression of CXCR4, an experimentally validated target of miR-139-5p. Correspondingly, treatment with high glucose resulted in a significant increase in THP-1 cell migration towards SDF-1, a cognate ligand for CXCR4. MiR-139-5p overexpression inhibited high glucose-induced CXCR4 expression, leading to reduced cell migration towards SDF-1. High glucose did not affect THP-1 monocyte growth. In conclusion, the miR-139-5p-CXCR4 axis may play a role in high glucose-induced inflammation by regulating monocyte migration.

**Keywords** Diabetes, Monocyte, Inflammation, microRNA, Cell migration

Global diabetes prevalence has been increasing. It was estimated that there were 529 million people with diabetes worldwide in 2021; this number was projected to exceed one billion by 2050<sup>1</sup>. Inflammation is involved in the pathogenesis of the most common types of diabetes, namely type 1, type 2 and gestational diabetes<sup>2–5</sup>. Monocytes, a critical component of the innate immune system, play a key role in propagating inflammation under hyperglycemic conditions<sup>6–9</sup>.

MicroRNAs (miRNAs) are a class of short, noncoding, single-stranded RNA molecules approximately 22 nucleotides in length; they regulate gene expression post-transcriptionally by binding to the 3'-untranslated region of mRNAs<sup>10,11</sup>. Since their discovery over three decades ago<sup>12,13</sup>, miRNAs have been extensively explored for their involvement in the pathophysiology of various diseases, including cancer<sup>14–16</sup>, cardiovascular disease<sup>17–20</sup>, and diabetes<sup>21–23</sup>. Many clinical studies of diabetic patients have shown alterations in circulating miRNAs and the altered miRNAs were investigated as potential disease biomarkers<sup>24–28</sup>. It has also been shown that miRNAs participate in various aspects of the actions of insulin that include insulin production, resistance, and cellular signaling<sup>29–31</sup>. In addition, miRNAs are implicated in the endothelial dysfunction observed in diabetes<sup>32–34</sup>. In contrast, although a few studies have described miRNA dysregulation in monocytes from patients with type 2 diabetes, they did not examine, or show, miRNA regulation of monocyte inflammatory activity<sup>35–37</sup>. This study aimed to investigate miRNA dysregulation in THP-1 monocytes in the presence of high glucose and its effects on cellular inflammatory function. The following miRNAs, i.e., miR-19a, miR-24, let-7b, miR-22, miR-139-5p and

<sup>1</sup>Department of Geriatric Endocrinology, The First Affiliated Hospital of Zhengzhou University, Zhengzhou, China. <sup>2</sup>Division of Cardiology, Keenan Research Center for Biomedical Science, St. Michael's Hospital, Unity Health Toronto, University of Toronto, Toronto, ON, Canada. ✉email: Qiuwang.Zhang@unityhealth.to; Michael.Kutryk@unityhealth.to

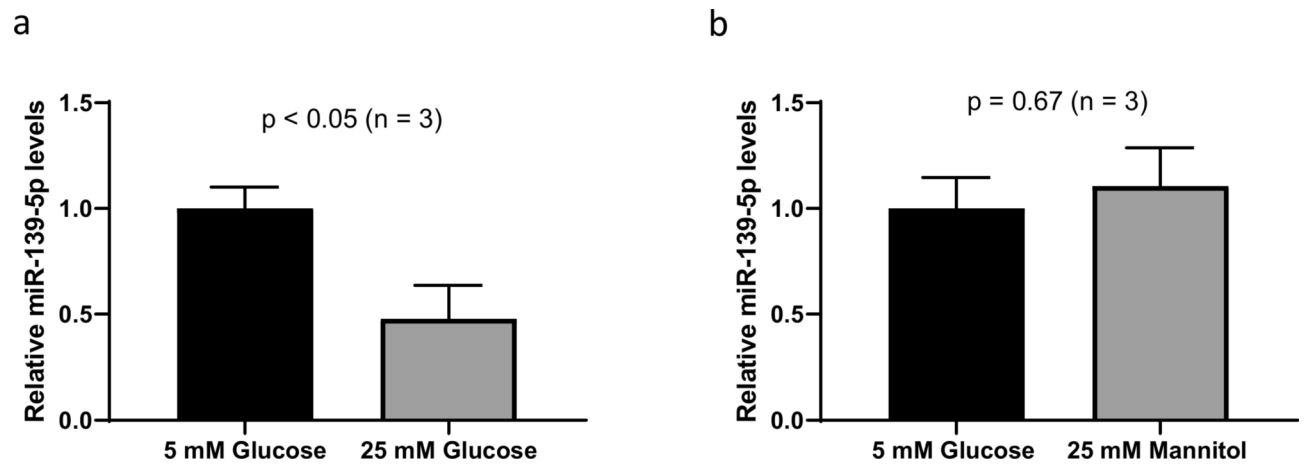


**Fig. 1.** MiRNA measurement. RT-qPCR analysis revealed a significantly lower level of miR-139-5p in THP-1 cells treated with 25 mM glucose than in those treated with 5 mM glucose (panel a). In contrast, there was no significant difference in miR-139-3p levels between 5 mM glucose- and 25 mM mannitol-treated cells (panel b).

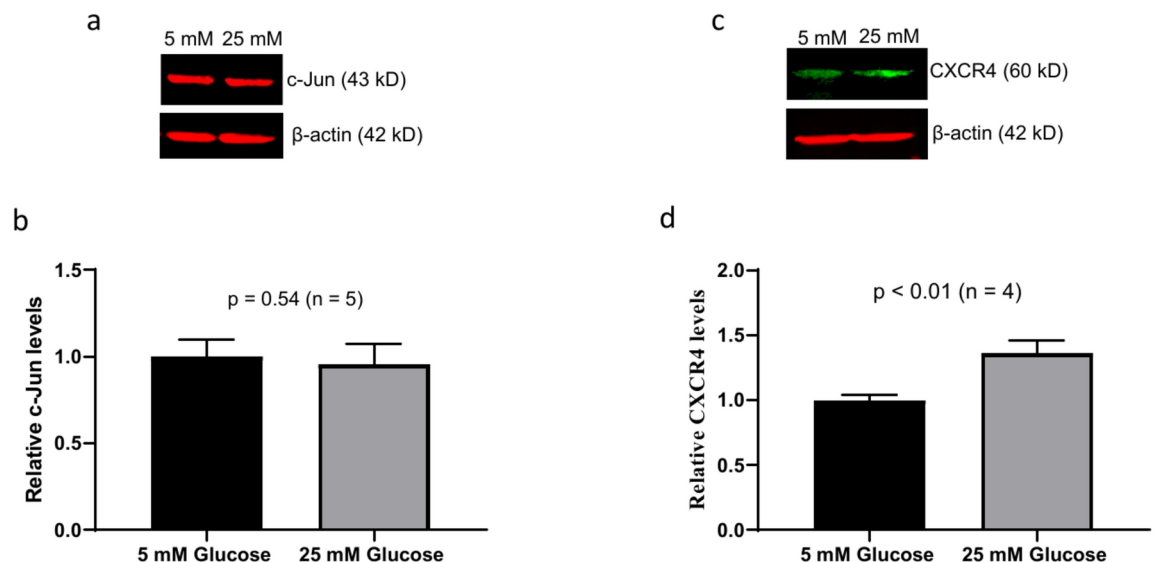


**Fig. 2.** c-Jun and CXCR4 protein measurement. c-Jun and CXCR4 levels were determined by Western blotting. While no significant difference was found in c-Jun levels between THP-1 cells treated with 5 mM and 25 mM glucose (panels a and b), CXCR4 levels were significantly higher in the 25 mM glucose cell group than in the 5 mM glucose cell group (panels c and d).

miR-152 were chosen for this study as they have been shown to regulate monocyte/macrophage inflammatory reactions<sup>38–47</sup>.

## Results

### miR-139-5p and its target CXCR4 were dysregulated by high glucose

Among the miRNAs assayed, miR-139-5p was significantly downregulated in THP-1 cells by 25 mM glucose (Fig. 1a), while expression of other miRNAs did not alter substantially (Supplementary Fig. 1). There was no marked difference in miR-139-5p levels between cells treated with 5 mM glucose and cells treated with 25 mM mannitol (Fig. 1b). CXCR4 and c-Jun, two key regulators of monocyte inflammatory activity, are predicted targets of miR-139-5p (<https://mirdb.org/cgi-bin/search.cgi?searchType=miRNA&full=mirbase&searchBox=MIMAT0000250>). Therefore, they were chosen for further analysis. Western blot analysis showed that high glucose did not affect c-Jun expression but markedly increased CXCR4 production (Fig. 2).

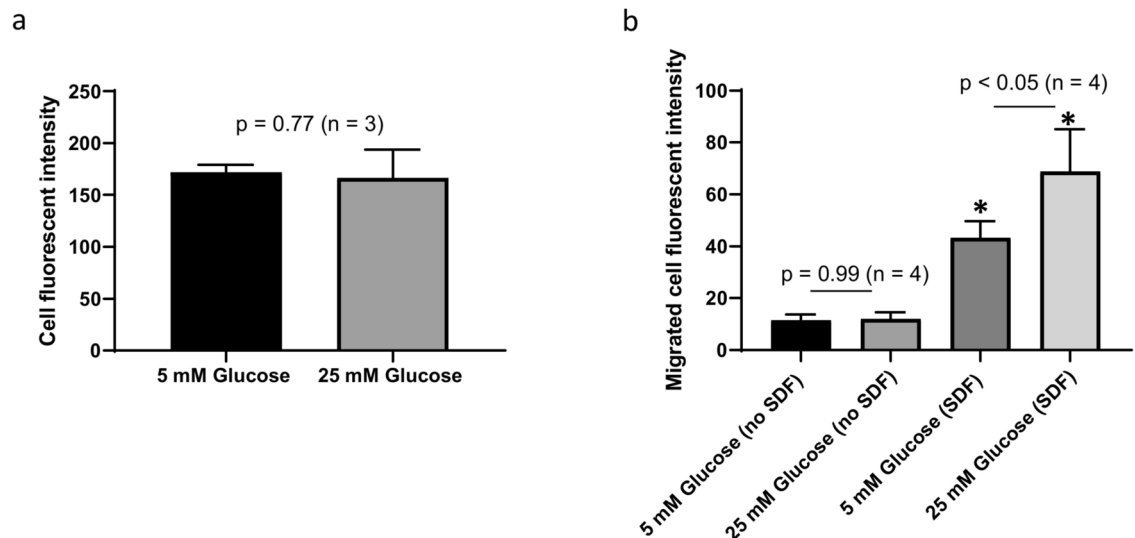


**Fig. 3.** THP-1 cell growth and migration assessment. Cell growth and migration were assayed by Calcein-AM staining as described in the Materials and Methods section. As shown in panel a, in cell growth analysis, the fluorescent intensity between the two groups of cells were not significantly different. As shown in panel b, in the presence of SDF-1, the fluorescent intensity of migrated cells was significantly greater in the 25 mM glucose cell group than in the 5 mM glucose cell group. \* indicates  $p < 0.001$  compared to cells treated with either 5 mM or 25 mM glucose in the absence of SDF-1.

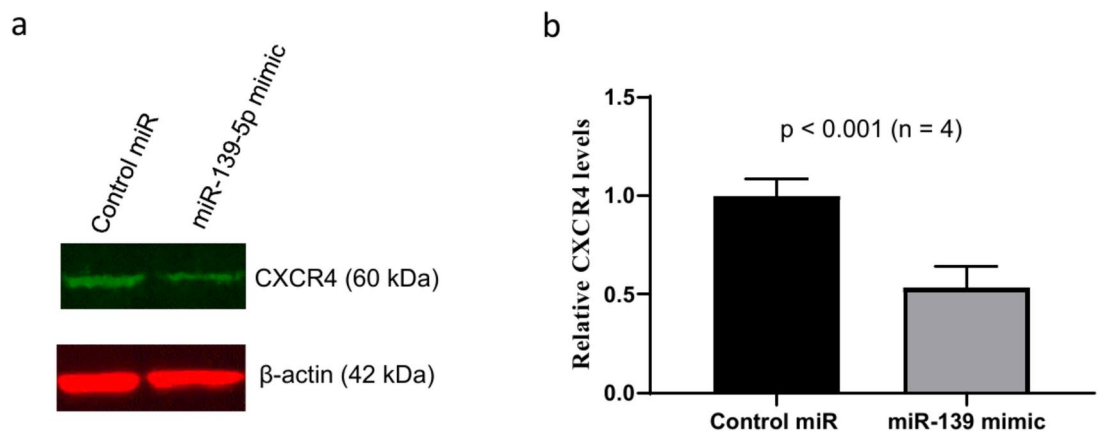


**Fig. 4.** CXCR4 protein measurement after miR-139-5p overexpression. CXCR4 protein levels were analyzed by Western blotting. Panel a shows a representative blot for CXCR4. CXCR4 protein levels were significantly lower in miR-139-5p mimic transfected cells than in control cells (panel b).

### High glucose did not affect THP-1 growth but enhanced cell migration towards SDF-1 (CXCL12)

As shown in Fig. 3a, there were no significant differences in cell growth between 5 and 25 mM glucose treated cells. We further looked into the ability of cell migration towards SDF-1, a cognate ligand for CXCR4. Of interest, treatment with 25 mM glucose led to a remarkable increase in THP-1 cell migration towards SDF-1 (Fig. 3b).

### Overexpression of miR-139-5p resulted in inhibition of CXCR4 production in the presence of high glucose

We successfully introduced miR-139-5p in THP-1 cells as RT-qPCR showed a significant increase of miR-139-5p levels after cell transfection with miR-139-5p mimic oligonucleotides (Supplementary Fig. 2). With the overexpression of miR-139-5p, CXCR4 protein levels decreased in the presence of high glucose as detected by Western blotting (panels a and b of Fig. 4).

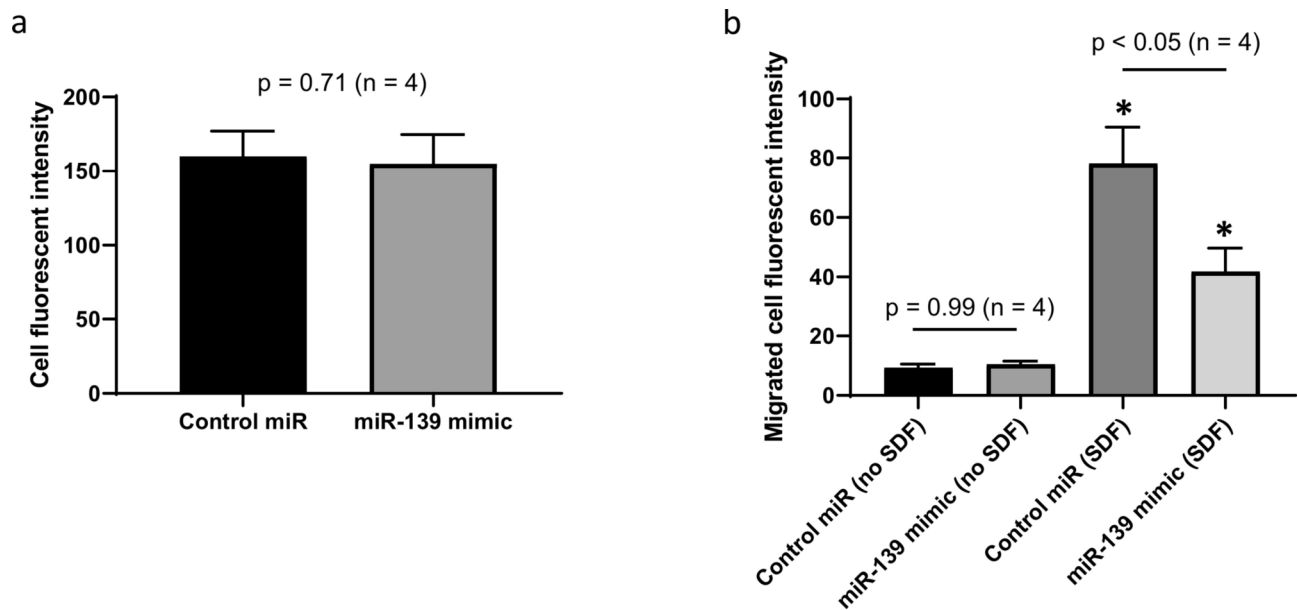


**Fig. 5.** THP-1 cell growth and migration assessment after miR-139-5p overexpression. Cell growth analysis showed that the Calcein-AM fluorescent intensity was not significantly different between the two groups of cells (panel a). Cell migration analysis showed that, in the presence of SDF-1, a significantly lower level of fluorescent intensity was detected for migrated cells overexpressing miR-139-5p compared to control cells (panel b). \*indicates  $p < 0.001$  compared to miR-139-5p overexpression cells or control cells in the absence of SDF-1.

### Overexpression of miR-139-5p suppressed THP-1 migration towards SDF-1

We examined if overexpression of miR-139-5p had an impact on cell growth. As shown in Fig. 5a, introduction of miR-139-5p into THP-1 cells did not significantly affect cell growth in the presence of 25 mM glucose. However, THP-1 cells overexpressing miR-139-5p showed a remarkable reduction in migration towards SDF-1 (Fig. 5b).

### Discussion

In this study, we report the following findings: (1) high glucose downregulated miR-139-5p in THP-1 monocytes, (2) the decrease of miR-139-5p in the presence of high glucose was associated with the upregulation of CXCR4, a target of miR-139-5p, (3) high glucose treatment led to a significant increase in THP-1 cell migration towards SDF-1, a cognate ligand for CXCR4, but did not affect cell growth, (4) transfection with miR-139-5p mimics significantly increased miR-139-5p levels in THP-1 monocytes and decreased CXCR4 protein production, and (5) miR-139-5p overexpression reduced THP-1 cell migration towards SDF-1.

Monocyte activation and increased production of pro-inflammatory cytokines are well-recognized contributors to diabetes<sup>6,48–50</sup>. It was shown that monocytes from patients with type 2 diabetes expressed TNF- $\alpha$  and IL-8 detectable by RT-PCR, while monocytes from healthy individuals did not<sup>48</sup>. Cipolletta et al. demonstrated that monocyte chemoattractant protein-1 was increased in monocytes from both type 1 and type 2 diabetic patients compared with control monocytes<sup>49</sup>. Enhanced adhesion to endothelial cells was observed for monocytes from diabetic patients and for high glucose treated THP-1 monocytes as well<sup>49,50</sup>. Nandy et al. reported that high glucose promoted monocyte migration<sup>50</sup>. Despite the advances of our knowledge about monocyte participation in diabetes, how monocyte-induced inflammation contributes to the pathogenesis of diabetes is not fully understood<sup>6</sup>. MiRNAs have been widely studied in diabetes<sup>24–37</sup>, however, their involvement in high glucose induced monocyte inflammatory response is poorly described. We selected miR-19a, miR-24, let-7b, miR-22, miR-139p-5p and miR-152 for investigation as previous studies have shown that these miRNAs regulate monocyte/macrophage inflammatory reactions<sup>38–47</sup>. Busch et al. revealed that the inhibition of miR-19a by antagomirs substantially increased lipoxygenase (5-LO) protein production in human Mono Mac 6 monocytes<sup>39</sup>. 5-LO is a key enzyme in the biosynthesis of leukotrienes, potent mediators of acute and chronic inflammation<sup>51</sup>. MiR-24 inhibits pro-inflammatory cytokine secretion in response to LPS in human macrophages<sup>41</sup>. Let-7b facilitates Mycobacterium tuberculosis survival in human THP-1 monocytes by downregulating Fas<sup>42</sup>. In another study, let-7b mitigated tumor inflammation by the inhibition of IL-6 in mouse macrophages<sup>43</sup>. Chen et al. observed a decrease of miR-22 in monocytes from patients with coronary heart disease. Furthermore, reduced miR-22 expression led to increased production of monocyte chemoattractant protein-1, that may contribute to atherogenesis<sup>44</sup>. MiR-152 represses IL-1, IL-6 and TNF- $\alpha$  expression induced by ox-LDL in mouse RAW264.7 macrophages<sup>47</sup>. Despite these findings, miR-19a, miR-24, let-7b, miR-22, and miR-152 were not found to be dysregulated in THP-1 monocytes by high glucose in the present study.

The role of miR-139-5p in inflammation has been documented<sup>46,52</sup>. Xu et al. reported that Salmonella infection of RAW264.7 macrophages induced IL-1 $\beta$  and TNF- $\alpha$  expression associated with decreased miR-

139-5p production<sup>46</sup>. The overexpression of miR-139-5p downregulated IL-1 $\beta$  and TNF- $\alpha$  in RAW264.7 macrophages exposed to Salmonella. Furthermore, the luciferase reporter assay validated the TNF-receptor associated factor 6 (TRAF6) as a target of miR-139-5p. Accordingly, RAW264.7 cells overexpressing miR-139-5p resulted in decreased TRAF6 protein expression. Of note, RAW264.7 macrophages transfected with a TRAF6 plasmid produced higher levels of IL-1 $\beta$  and TNF- $\alpha$  than cells transfected with a control plasmid. These data indicate that miR-139-5p inhibits Salmonella induced IL-1 $\beta$  and TNF- $\alpha$  expression in RAW264.7 macrophages by targeting TRAF6<sup>46</sup>. A recent study found that miR-139-5p was enriched in extracellular vesicles derived from human umbilical cord mesenchymal stromal cells treated with IL-1 $\beta$  and TNF- $\alpha$  in combination. These extracellular vesicles, when co-cultured with human peripheral mononuclear cells, led to increased expression of the anti-inflammatory protein FoxP3 in mononuclear cells<sup>52</sup>. In the present study, we observed miR-139-5p downregulation by high glucose in THP-1 cells associated with elevated CXCR4 production and enhanced cell migration towards SDF-1. Moreover, overexpression of miR-139-5p in high glucose treated THP-1 cells led to decreased CXCR4 expression and cell migration. Our findings are consistent with published data, indicating an anti-inflammatory role of miR-139-5p.

We detected decreased miR-139-5p levels in THP-1 cells treated with high glucose. CXCR4 and c-Jun, two critical modulators of monocyte inflammatory activity<sup>53–57</sup>, have been experimentally validated to be targets of miR-139-5p<sup>58,59</sup>. CXCR4 promotes monocyte migration via its cognate ligand SDF-1, to contribute to inflammation<sup>53,54</sup>. c-Jun, a key component of the transcript factor AP-1 complex, regulates inflammatory cytokine expression in monocytes<sup>55–57</sup>. Western blot analysis revealed that high glucose increased CXCR4 but did not alter c-Jun expression. Accordingly, THP-1 cells treated with high glucose showed a greater level of migration towards SDF-1 than control cells. These effects were reversed by miR-139-5p overexpression.

Increased monocyte migration leads to monocyte accumulation in various organs and tissues involved in the pathogenesis of diabetes, including the pancreas, the vascular endothelium, and adipose tissue<sup>60–63</sup>. Under hyperglycemia, the recruited monocytes differentiate into macrophages, releasing pro-inflammatory cytokines and promoting inflammation<sup>64</sup>. An increased number of macrophages, due to enhanced monocyte migration, is observed in the islets of patients with type 2 diabetes compared to non-diabetic controls, which leads to an increase in  $\beta$  cell apoptosis and a reduction in insulin production<sup>60,61</sup>. Atherosclerosis is a major vascular complication of diabetes. Monocytes enter the sub-endothelial space and differentiate into macrophages, driving the development of atherosclerosis. A postmortem study showed that patients with diabetes and coronary artery disease (CAD) had a significantly higher number of macrophages in the vascular intima compared to CAD patients without diabetes<sup>62</sup>. Enhanced macrophage infiltration into the adipose tissue causing insulin resistance and diabetes has also been well documented<sup>63</sup>. Taken together, these findings suggest that increased monocyte migration plays a critical role in the development and progression of diabetes and its complications.

Of interest, animal and clinical studies have shown elevated levels of SDF-1 in diabetes. In a mouse model of diabetes, increased SDF-1 expression was found in glomerular podocytes and distal nephrons in the diabetic mice, but not in control mice<sup>65</sup>. In patients with type 2 diabetes, blood levels of SDF are significantly higher compared to those in healthy individuals<sup>66,67</sup>. Butler et al. reported that SDF-1 was detectable in vitreous samples from patients with diabetic retinopathy but not in those from non-diabetic patients<sup>68</sup>. These findings, along with our data, suggest that the SDF-1/CXCR4 system may contribute to increased monocyte infiltration into organs such as eyes and kidneys, promoting the progression of diabetes and its complications.

In conclusion, high glucose downregulates miR-139-5p in THP-1 cells, that is associated with increased CXCR4 expression and cell migration towards SDF-1. Overexpression of miR-139-5p reverses the effects of high glucose. Therefore, the miR-139-5p-CXCR4 axis may play a role in high glucose-induced inflammation by regulating monocyte migration.

## Materials and methods

### Materials

RPMI 1640 medium with 25 mM glucose (Cat # A1049101), RPMI 1640 medium without glucose (Cat # 11,879,020), fetal bovine serum (FBS, Cat # A3840301), Lipofectamine RNAiMAX Transfection Reagent (Cat # 13,778,075), OPTI-MEM medium (Cat # 31,985,062), TaqMan MicroRNA Assay Kit (Cat # 4,427,975), miR-139-5p Mimic (Cat # 4,464,066, Assay ID: MC11749), miRNA Mimic Negative Control (Cat # 4,464,058), TaqMan miRNA Reverse Transcription Kit (Cat # 4,366,596), TaqMan Fast Advanced Master Mix (Cat # 4,444,557), and c-Jun monoclonal antibody (Cat # MA5-15,881) were obtained from Life Technologies (Burlington, ON, Canada). Qiagen RNeasy Mini Kit (Cat # 217,004) was purchased from Qiagen (Toronto, ON, Canada). Anti-CXCR4 antibody (Cat # 64,837) was provided by Cell Signaling Technology (Whitby, ON, Canada). Anti-beta-actin antibody (cat # A5316), Calcein-AM fluorescence dye (Cat # C0875-5G), glucose (Cat # G7021) and mannitol (Cat # M4125) were purchased from Sigma-Aldrich Canada Co. (Oakville, ON, Canada). Fluorescence labeled IRDye 800CW goat anti-rabbit secondary antibody (Cat # 926–32,211) and IRDye 680CW goat anti-mouse secondary antibody (Cat # 926–68,070) were purchased from LI-COR Corporate (Lincoln, NE, USA). Transwell Boyden Chamber Inserts (8  $\mu$ m) were obtained from BD Biosciences (Mississauga, ON, Canada).

### THP-1 cell culture and treatment

Human THP-1 monocytes (Cat # TIB-202, ATCC) were maintained in RPMI 1640 medium with 25 mM glucose and 10% FBS. For treatment with high glucose, cells were pelleted by centrifugation, suspended at a density of 1 million/mL with glucose-free RPMI 1640 medium containing 1% FBS, and seeded into a 12-well plate (1 million cells/well) followed by addition of glucose at a final concentration of 5 mM (normal glucose) or 25 mM (high glucose). Cells were cultured for 24 h followed by replacement of spent medium with fresh RPMI 1640 medium containing 1% FBS and 5 mM or 25 mM glucose. After another 24 h of culture, cells were harvested for analyses.



For miRNA measurement, cells were also treated with 25 mM mannitol for 48 h, with fresh mannitol-containing medium replaced every 24 h.

### RNA extraction

After THP cells were treated with different concentrations of glucose or 25 mM mannitol for 48 h, cellular RNA was extracted using a Qiagen RNeasy Mini Kit as described elsewhere<sup>69</sup>. Briefly, THP-1 cells from each well were collected into a microtube and pelleted with centrifugation. After removal of the supernatant, cells were lysed with 700  $\mu$ L of Qiazol lysis reagent followed by addition of 140  $\mu$ L of chloroform. The mixture was then centrifuged at  $12,000 \times g$  for 15 min at 4 °C. After centrifugation, 200–300  $\mu$ L of the upper aqueous layer containing RNA was carefully extracted, mixed with 1.5 volumes of 100% ethanol and transferred into an RNeasy Mini column. Subsequently, the column was centrifuged at  $10,000 \times g$  for 15 s to allow for RNA binding. After two washes of bound RNA with 500  $\mu$ L of Buffer RPE each time by centrifugation at  $10,000 \times g$  for 15 s, RNA was eluted with 30  $\mu$ L of RNase-free water by centrifugation at  $10,000 \times g$  for 1 min. RNA was quantified using a NanoDrop 2000 spectrophotometer and stored at –80 °C until analyzed.

### Reverse transcription-quantitative polymerase chain reaction (RT-qPCR)

RT-qPCR was performed to measure miRNAs with U6 RNA serving as an endogenous control as described elsewhere<sup>69</sup>. Briefly, RT was done with the TaqMan miRNA Reverse Transcription Kit in a total reaction volume of 15  $\mu$ L, containing 4  $\mu$ L (20 ng) RNA, 1.5  $\mu$ L  $10 \times$  RT buffer, 0.2  $\mu$ L 100 mM dNTP, 3  $\mu$ L  $5 \times$  individual miRNA specific primer, 1  $\mu$ L MultiScribe Reverse Transcriptase, 1  $\mu$ L RNase inhibitor and 4.4  $\mu$ L nuclease-free  $H_2O$ . RT reaction was completed by incubating the mixture at 16 °C for 30 min, 42 °C for 30 min and 85 °C for 5 min. For qPCR, 1  $\mu$ L of RT product was mixed with 0.5  $\mu$ L  $20 \times$  TaqMan MicroRNA assay primer, 5  $\mu$ L  $2 \times$  TaqMan Fast Advanced Master Mix and 3.5  $\mu$ L of nuclease-free  $H_2O$ . PCR was performed on a QuantStudio 7 Flex Real-Time PCR System (Life Technologies) according to the following thermocycling protocol: 95 °C for 20 s and 40 cycles of 95 °C for 1 s and 60 °C for 20 s. The fold change of the miRNA level in the presence of high glucose over that of normal glucose was calculated using the  $2^{-\Delta\Delta C_t}$  method<sup>70</sup>.

### Western blotting

CXCR4 and c-Jun protein levels were determined by Western blot analysis as described elsewhere<sup>71</sup>. Briefly, cellular protein was prepared with RIPA lysis buffer, separated by SDS-PAGE and electrically transferred onto a nitrocellulose membrane. The membrane was blocked in TBS-T buffer (50 mM TrisHCl, 150 mM NaCl, pH 7.5, 0.1% Tween-20) containing 5% skimmed milk at room temperature for 1 h followed by incubation with the primary antibodies (1:1000 dilution for c-Jun and CXCR4 antibodies and 1:5000 for beta-actin antibody) at 4 °C overnight. After three washes with TBS-T buffer, the membrane was incubated at room temperature in the dark for one hour with fluorescence-labeled secondary antibodies (1:5000 dilution). Subsequently, three washes of the membrane with TBS-T buffer were done and the specific protein band was visualized using the Odyssey Fluorescence Imaging System (LI-COR Corporate). Fluorescence intensity of the protein band was analysed using the Empiria Studio Software (LI-COR Corporate). The ratio of target protein fluorescence intensity over beta actin fluorescence intensity in the experimental cells was compared with that of control cells. The ratio in the control cells was taken to be 1.0.

### miRNA mimic transfection and cell treatment

Cell transfection was done in a 12-well plate as follows: 2  $\mu$ L of miR-139-5p mimics or mimic control (both at a stock concentration of 10  $\mu$ M) and 2  $\mu$ L of Lipofectamine RNA iMAX transfection reagent were diluted in 125  $\mu$ L OPTI-MEM medium, respectively; the diluted reagent and miRNA mimics were then mixed and incubated at room temperature for 15 min. After incubation, 250  $\mu$ L of the mixture was added to each well of 1.75 mL THP-1 cells at a density of 1 million cells/mL prepared with fresh RPMI 1640 medium with 25 mM glucose and 10% FBS. After culture for 24 h, both control and miR-139-5p mimic transfected cells were treated with high glucose for 48 h as described above for analyses.

### Cell proliferation assay

THP-1 cells were suspended at a density of 1 million/mL with glucose-free RPMI 1640 medium containing 1% FBS, seeded into a 24-well plate (0.5 mL cells/well) and treated with normal or high glucose for 48 h as described above. Afterwards, to stain live cells, the fluorescent dye Calcein-AM was added to cells at a final concentration of 1  $\mu$ M and cells were maintained in culture for 30 min. Finally, the fluorescent intensity was measured (excitation at 485 nm and emission at 538 nm) and compared between different groups of cells.

### Cell migration assay

A Boyd chamber cell migration assay was used to examine THP-1 cell response towards the chemoattractant SDF-1, the cognate ligand for CXCR4. THP-1 cells were stained with Calcein-AM for 30 min, washed once with PBS and suspended at a density of 1 million/mL in migration medium, i.e., glucose- and serum-free RPMI 1640 medium. The Transwell Boyden Chamber Inserts were placed in a 24-well plate (one insert/well) and 0.3 mL of cells were added into the top chamber of each insert while 500  $\mu$ L of migration medium containing SDF-1 (100 ng/mL) or 500  $\mu$ L of migration medium alone as control was added into the lower chamber. After incubation at 37 °C for 3 h, the inserts were removed and the fluorescent intensity of cells migrated in the lower chamber was measured and compared between different groups of cells.

## Statistical analysis

Data were presented as Mean  $\pm$  SD. Variables between two groups were analyzed with the student's *t* test; cell migration data were analyzed with the ANOVA with post-hoc Tukey test using the GraphPad Prism 8 software (GraphPad Software Inc., San Diego, CA, USA). A *p*-value  $< 0.05$  was considered statistically significant.

## Data availability

Data is provided within the manuscript or supplementary information files.

Received: 3 October 2024; Accepted: 18 February 2025

Published online: 25 February 2025

## References

1. GBD 2021 Diabetes Collaborators. Global, regional, and national burden of diabetes from 1990 to 2021, with projections of prevalence to 2050: A systematic analysis for the Global Burden of Disease Study 2021. *Lancet*. **402**, 203–234 (2023).
2. Tsalamandris, S. et al. The role of inflammation in diabetes: Current concepts and future perspectives. *Eur. Cardiol.* **14**, 50–59 (2019).
3. Donath, M. Y. & Shoelson, S. E. Type 2 diabetes as an inflammatory disease. *Nat. Rev. Immunol.* **11**, 98–107 (2011).
4. Clark, M., Kroger, C. J. & Tisch, R. M. Type 1 diabetes: A chronic anti-self-inflammatory response. *Front. Immunol.* **8**, 1898 (2017).
5. Pantham, P., Aye, I. L. & Powell, T. L. Inflammation in maternal obesity and gestational diabetes mellitus. *Placenta*. **36**, 709–715 (2015).
6. Mokgalaboni, K. et al. Monocyte-mediated inflammation and cardiovascular risk factors in type 2 diabetes mellitus: A systematic review and meta-analysis of pre-clinical and clinical studies. *JRSM Cardiovasc. Dis.* **9**, 2048004019900748 (2020).
7. Pant, T. et al. Monocytes in type 1 diabetes families exhibit high cytolytic activity and subset abundances that correlate with clinical progression. *Sci. Adv.* **10**, eadn2136 (2024).
8. Thiem, K. et al. A high glycemic burden relates to functional and metabolic alterations of human monocytes in patients with type 1 diabetes. *Diabetes*. **69**, 2735–2746 (2020).
9. Hatanaka, E., Monteagudo, P. T., Marrocos, M. S. & Campa, A. Neutrophils and monocytes as potentially important sources of proinflammatory cytokines in diabetes. *Clin. Exp. Immunol.* **146**, 443–447 (2006).
10. Shang, R., Lee, S., Senavirathne, G. & Lai, E. C. microRNAs in action: Biogenesis, function and regulation. *Nat. Rev. Genet.* **24**, 816–833 (2023).
11. O'Brien, J., Hayder, H., Zayed, Y. & Peng, C. Overview of microRNA biogenesis, mechanisms of actions, and circulation. *Front. Endocrinol. (Lausanne)* **9**, 402 (2018).
12. Lee, R. C., Feinbaum, R. L. & Ambros, V. T. *Elegans* heterochronic gene lin-4 encodes small RNAs with antisense complementarity to lin-14. *Cell* **75**, 843–854 (1993).
13. Wightman, B., Ha, I. & Ruvkun, G. Posttranscriptional regulation of the heterochronic gene lin-14 by lin-4 mediates temporal pattern formation in *C. elegans*. *Cell* **75**, 855–862 (1993).
14. Smolarz, B. et al. miRNAs in cancer (review of literature). *Int. J. Mol. Sci.* **23**, 2805 (2022).
15. Reddy, K. B. MicroRNA (miRNA) in cancer. *Cancer Cell Int.* **15**, 38 (2015).
16. Jansson, M. D. & Lund, A. H. MicroRNA and cancer. *Mol. Oncol.* **6**, 590–610 (2012).
17. Sessa, F. et al. MiRNA dysregulation in cardiovascular diseases: Current opinion and future perspectives. *Int. J. Mol. Sci.* **24**, 5192 (2023).
18. Peters, L. J. F. et al. Small things matter: Relevance of microRNAs in cardiovascular disease. *Front. Physiol.* **11**, 793 (2020).
19. Johnson, J. L. Elucidating the contributory role of microRNA to cardiovascular diseases (a review). *Vascul. Pharmacol.* **114**, 31–48 (2019).
20. Romaine, S. P., Tomaszewski, M., Condorelli, G. & Samani, N. J. MicroRNAs in cardiovascular disease: An introduction for clinicians. *Heart*. **101**, 921–928 (2015).
21. Paschou, S. A. et al. The Role of microRNAs in the development of type 2 diabetes complications. *Curr. Pharm. Des.* **26**, 5969–5979 (2020).
22. Kim, M. & Zhang, X. The profiling and role of miRNAs in diabetes mellitus. *J. Diabetes Clin. Res.* **1**, 5–23 (2019).
23. Tang, X., Tang, G. & Ozcan, S. Role of microRNAs in diabetes. *Biochim. Biophys. Acta*. **1779**, 697–701 (2008).
24. Erener, S. et al. Profiling of circulating microRNAs in children with recent onset of type 1 diabetes. *JCI Insight*. **2**, e89656 (2017).
25. Seyhan, A. A. et al. Pancreas-enriched miRNAs are altered in the circulation of subjects with diabetes: A pilot cross-sectional study. *Sci. Rep.* **6**, 31479 (2016).
26. Zhang, T. et al. Circulating miR-126 is a potential biomarker to predict the onset of type 2 diabetes mellitus in susceptible individuals. *Biochem. Biophys. Res. Commun.* **463**, 60–63 (2015).
27. Kong, L. et al. Significance of serum microRNAs in pre-diabetes and newly diagnosed type 2 diabetes: A clinical study. *Acta Diabetol.* **48**, 61–69 (2011).
28. Zampetaki, A. et al. Plasma microRNA profiling reveals loss of endothelial miR-126 and other microRNAs in type 2 diabetes. *Circ. Res.* **107**, 810–817 (2010).
29. Poy, M. N. et al. A pancreatic islet-specific microRNA regulates insulin secretion. *Nature* **432**, 226–230 (2004).
30. Chakraborty, C., Doss, C. G., Bandyopadhyay, S. & Agoramoorthy, G. Influence of miRNA in insulin signaling pathway and insulin resistance: Micro-molecules with a major role in type-2 diabetes. *RNA* **5**, 697–712 (2014).
31. Nigi, L. et al. MicroRNAs as regulators of insulin signaling: Research updates and potential therapeutic perspectives in type 2 diabetes. *Int. J. Mol. Sci.* **19**, 3705 (2018).
32. Fluit, M. B., Mohit, N., Gambhir, K. K. & Nunlee-Bland, G. To the future: The role of exosome-derived microRNAs as markers, mediators, and therapies for endothelial dysfunction in type 2 diabetes mellitus. *J. Diabetes Res.* **2022**, 5126968 (2022).
33. Silambarasan, M. et al. MicroRNAs in hyperglycemia induced endothelial cell dysfunction. *Int. J. Mol. Sci.* **17**, 518 (2016).
34. Zhang, H. N. et al. Endothelial dysfunction in diabetes and hypertension: Role of microRNAs and long non-coding RNAs. *Life Sci.* **213**, 258–268 (2018).
35. Parker, D. C. et al. Monocyte miRNAs are associated with type 2 diabetes. *Diabetes*. **71**, 853–861 (2022).
36. Wang, S. S. et al. Expression of miR-18a and miR-34c in circulating monocytes associated with vulnerability to type 2 diabetes mellitus and insulin resistance. *J. Cell. Mol. Med.* **21**, 3372–3380 (2017).
37. Baldeón, R. L. et al. Type 2 diabetes monocyte microRNA and mRNA expression: Dyslipidemia associates with increased differentiation-related genes but not inflammatory activation. *PLoS One*. **10**, e0129421 (2015).
38. Chen, H. et al. MicroRNA-19a promotes vascular inflammation and foam cell formation by targeting HBP-1 in atherosclerosis. *Sci. Rep.* **7**, 12089 (2017).
39. Busch, S. et al. 5-lipoxygenase is a direct target of miR-19a-3p and miR-125b-5p. *J. Immunol.* **194**, 1646–1653 (2015).
40. Naqvi, A. R., Fordham, J. B. & Nares, S. miR-24, miR-30b, and miR-142-3p regulate phagocytosis in myeloid inflammatory cells. *J. Immunol.* **194**, 1916–1927 (2015).

41. Fordham, J. B., Naqvi, A. R. & Nares, S. miR-24 regulates macrophage polarization and plasticity. *J. Clin. Cell Immunol.* **6**, 362 (2015).
42. Tripathi, A., Srivastava, V. & Singh, B. N. hsa-let-7b-5p facilitates Mycobacterium tuberculosis survival in THP-1 human macrophages by Fas downregulation. *FEMS Microbiol. Lett.* **365**, fny040 (2018).
43. Li, D. et al. TLR4 signaling induces the release of microparticles by tumor cells that regulate inflammatory cytokine IL-6 of macrophages via microRNA let-7b. *Oncoimmunology* **1**, 687–693 (2012).
44. Chen, B. et al. miR-22 contributes to the pathogenesis of patients with coronary artery disease by targeting MCP-1: An observational study. *Medicine (Baltimore)* **95**, e4418 (2016).
45. Ghorbani, S. et al. Expression levels of miR-22, miR-30c, miR-145, and miR-519d and their possible associations with inflammatory markers among patients with coronary artery disease. *ARYA Atheroscler.* **18**, 1–10 (2022).
46. Xu, X. et al. MicroRNA-139-5p inhibits inflammatory and oxidative stress responses of Salmonella-infected macrophages through modulating TRAF6. *Pathog. Dis.* **79**, ftab018 (2021).
47. Wang, W. et al. MicroRNA-152 prevents the malignant progression of atherosclerosis via down-regulation of KLF5. *Biomed. Pharmacother.* **109**, 2409–2414 (2019).
48. Gacka, M. et al. Proinflammatory and atherogenic activity of monocytes in type 2 diabetes. *J. Diabetes Complicat.* **24**, 1–8 (2010).
49. Cipolletta, C., Ryan, K. E., Hanna, E. V. & Trimble, E. R. Activation of peripheral blood CD14+ monocytes occurs in diabetes. *Diabetes* **54**, 2779–2786 (2005).
50. Nandy, D., Janardhanan, R., Mukhopadhyay, D. & Basu, A. Effect of hyperglycemia on human monocyte activation. *J. Investig. Med.* **59**, 661–667 (2011).
51. Sasaki, F. & Yokomizo, T. The leukotriene receptors as therapeutic targets of inflammatory diseases. *Int. Immunol.* **31**, 607–615 (2019).
52. Hyland, M. et al. Extracellular vesicles derived from umbilical cord mesenchymal stromal cells show enhanced anti-inflammatory properties via upregulation of miRNAs after pro-inflammatory priming. *Stem Cell Rev. Rep.* **19**, 2391–2406 (2023).
53. Schiraldi, M. et al. HMGB1 promotes recruitment of inflammatory cells to damaged tissues by forming a complex with CXCL12 and signaling via CXCR4. *J. Exp. Med.* **209**, 551–563 (2012).
54. Mai, C. L. et al. CXCL12-mediated monocyte transmigration into brain perivascular space leads to neuroinflammation and memory deficit in neuropathic pain. *Theranostics* **11**, 1059–1078 (2021).
55. Kochumon, S. et al. IL-1 $\beta$ -induced CXCL10 expression in THP-1 monocytic cells involves the JNK/c-Jun and NF- $\kappa$ B-mediated signaling. *Pharmaceuticals (Basel)* **17**, 823 (2024).
56. Tuyt, L. M. et al. Extracellular-regulated kinase 1/2, Jun N-terminal kinase, and c-Jun are involved in NF- $\kappa$ B-dependent IL-6 expression in human monocytes. *J. Immunol.* **162**, 4893–4902 (1999).
57. Guha, M. & Mackman, N. LPS induction of gene expression in human monocytes. *Cell Signal.* **13**, 85–94 (2001).
58. Papargeli, I. et al. MicroRNA 139-5p coordinates APLNR-CXCR4 crosstalk during vascular maturation. *Nat. Commun.* **7**, 11268 (2016).
59. Jin, S. S. et al. Silencing lncRNA NEAT1 reduces nonalcoholic fatty liver fat deposition by regulating the miR-139-5p/c-Jun/SREBP-1c pathway. *Ann. Hepatol.* **27**, 100584 (2022).
60. Ehses, J. A. et al. Increased number of islet-associated macrophages in type 2 diabetes. *Diabetes* **56**, 2356–2370 (2007).
61. Richardson, S. J. et al. Islet-associated macrophages in type 2 diabetes. *Diabetologia* **52**, 1686–1688 (2009).
62. Burke, A. P. et al. Morphologic findings of coronary atherosclerotic plaques in diabetics: A postmortem study. *Arterioscler Thromb Vasc. Biol.* **24**, 1266–1271 (2004).
63. Surmi, B. K. & Hasty, A. H. Macrophage infiltration into adipose tissue: Initiation, propagation and remodeling. *Future Lipidol.* **3**, 545–556 (2008).
64. Moganti, K. et al. Hyperglycemia induces mixed M1/M2 cytokine profile in primary human monocyte-derived macrophages. *Immunobiology* **222**, 952–959 (2017).
65. Takashima, S. et al. Stromal cell-derived factor-1 is upregulated by dipeptidyl peptidase-4 inhibition and has protective roles in progressive diabetic nephropathy. *Kidney Int.* **90**, 783–796 (2016).
66. Derakhshan, R. et al. Increased circulating levels of SDF-1 (CXCL12) in type 2 diabetic patients are correlated to disease state but are unrelated to polymorphism of the SDF-1 $\beta$  gene in the Iranian population. *Inflammation* **35**, 900–904 (2012).
67. Nätyнки, A. et al. Use of gliptins reduces levels of SDF-1/CXCL12 in bullous pemphigoid and type 2 diabetes, but does not increase autoantibodies against BP180 in diabetic patients. *Front. Immunol.* **13**, 942131 (2022).
68. Butler, J. M. et al. SDF-1 is both necessary and sufficient to promote proliferative retinopathy. *J. Clin. Invest.* **115**, 86–93 (2005).
69. Cannavici, A., Zhang, Q. & Kutryk, M. J. B. The potential role of miRs-139-5p and -454-3p in endoglin-knockdown-induced angiogenic dysfunction in HUVECs. *Int. J. Mol. Sci.* **24**, 4916 (2023).
70. Livak, K. J. & Schmittgen, T. D. Analysis of relative gene expression data using real-time quantitative PCR and the 2(-delta delta C(T)) method. *Methods* **25**, 402–408 (2001).
71. Zhang, Q. et al. Endoglin deficiency impairs VEGFR2 but not FGFR1 or TIE2 activation and alters VEGF-mediated cellular responses in human primary endothelial cells. *Transl. Res.* **235**, 129–143 (2021).

## Acknowledgements

This work was supported by the Alayne Metrick Fund, Toronto, ON, Canada.

## Author contributions

WL: methodology, investigation, formal analysis, writing-first draft GX, GWC, and AB: methodology, investigation, formal analysis QZ: conceptualization, investigation, formal analysis, writing-first draft MJBK: conceptualization, formal analysis, writing-review and editing.

## Declarations

## Competing interests

The authors declare no competing interests.

## Additional information

**Supplementary Information** The online version contains supplementary material available at <https://doi.org/10.1038/s41598-025-91100-1>.

**Correspondence** and requests for materials should be addressed to Q.Z. or M.J.B.K.

**Reprints and permissions information** is available at [www.nature.com/reprints](http://www.nature.com/reprints).



**Publisher's note** Springer Nature remains neutral with regard to jurisdictional claims in published maps and institutional affiliations.

**Open Access** This article is licensed under a Creative Commons Attribution-NonCommercial-NoDerivatives 4.0 International License, which permits any non-commercial use, sharing, distribution and reproduction in any medium or format, as long as you give appropriate credit to the original author(s) and the source, provide a link to the Creative Commons licence, and indicate if you modified the licensed material. You do not have permission under this licence to share adapted material derived from this article or parts of it. The images or other third party material in this article are included in the article's Creative Commons licence, unless indicated otherwise in a credit line to the material. If material is not included in the article's Creative Commons licence and your intended use is not permitted by statutory regulation or exceeds the permitted use, you will need to obtain permission directly from the copyright holder. To view a copy of this licence, visit <http://creativecommons.org/licenses/by-nc-nd/4.0/>.

© The Author(s) 2025